

Supplementary Information

Thiolutin is a zinc chelator that inhibits the Rpn11 and other JAMM metalloproteases

Linda Lauinger^{1,2}, Jing Li³, Anton Shostak¹, Ibrahim Avi Cemel¹, Nati Ha^{1,4}, Yaru Zhang³, Philipp E. Merkl^{5,6}, Simon Obermeyer⁵, Nicolas Stankovic-Valentin⁷, Tobias Schafmeier^{1,8}, Walter J Wever⁹, Albert A Bowers⁹, Kyle P Carter¹⁰, Amy E Palmer¹⁰, Herbert Tschochner⁵, Frauke Melchior⁷, Raymond J Deshaies^{3,11}, Michael Brunner^{1*}, and Axel Diernfellner^{1*}

¹ Heidelberg University Biochemistry Center, Heidelberg, Germany

² present address: University of California Irvine, Department of Biological Chemistry, School of Medicine, 240D Med Sci I, Irvine, CA 92697–1700, USA

³ Division of Biology and Biological Engineering, California Institute of Technology, Pasadena, CA, USA

⁴ present address: German Cancer Research Center (DKFZ), Applied Bioinformatics, Heidelberg, Germany

⁵ Universität Regensburg, Biochemie Zentrum Regensburg, Lehrstuhl Biochemie III, Regensburg, Germany

⁶ present address: Dept. of Microbiology and Immunobiology, Harvard Medical School, Boston, MA, USA

⁷ Zentrum für Molekulare Biologie der Universität Heidelberg, Heidelberg University, DKFZ-ZMBH Alliance, Germany.

⁸ present address: Institute for Diabetes and Cancer IDC Helmholtz Center Munich, Neuherberg, Germany

⁹ Division of Chemical Biology and Medicinal Chemistry, University of North Carolina at Chapel Hill, Eshelman School of Pharmacy, Chapel Hill, North Carolina 27599, United States

¹⁰ Department of Chemistry and Biochemistry, BioFrontiers Institute, 3415 Colorado Ave, UCB 596, University of Colorado, Boulder, CO 80303, USA

¹¹ Howard Hughes Medical Institute

* Corresponding authors: axel.diernfellner@bzh.uni-heidelberg.de; michael.brunner@bzh.uni-heidelberg.de

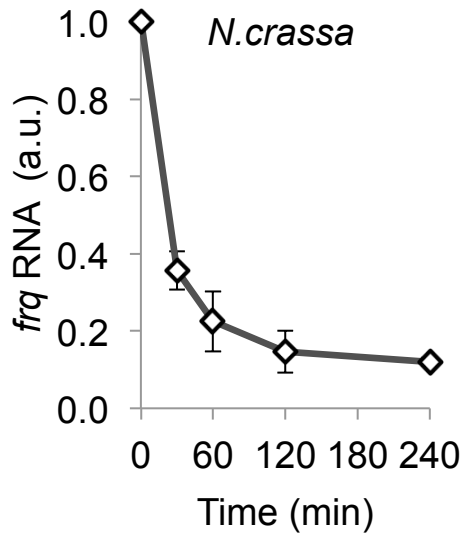
Supplementary Results

Supplementary Figures 1-10

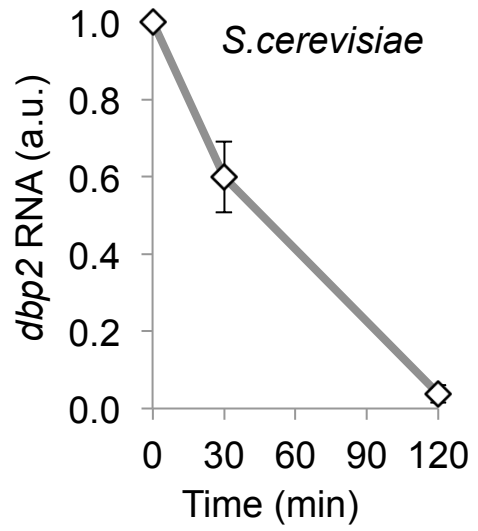
Supplementary Table

Supplementary Figure Legends

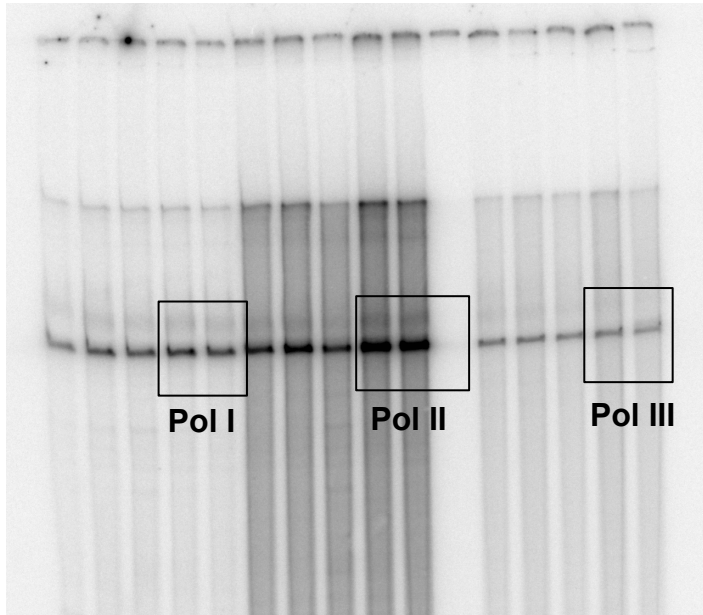
a



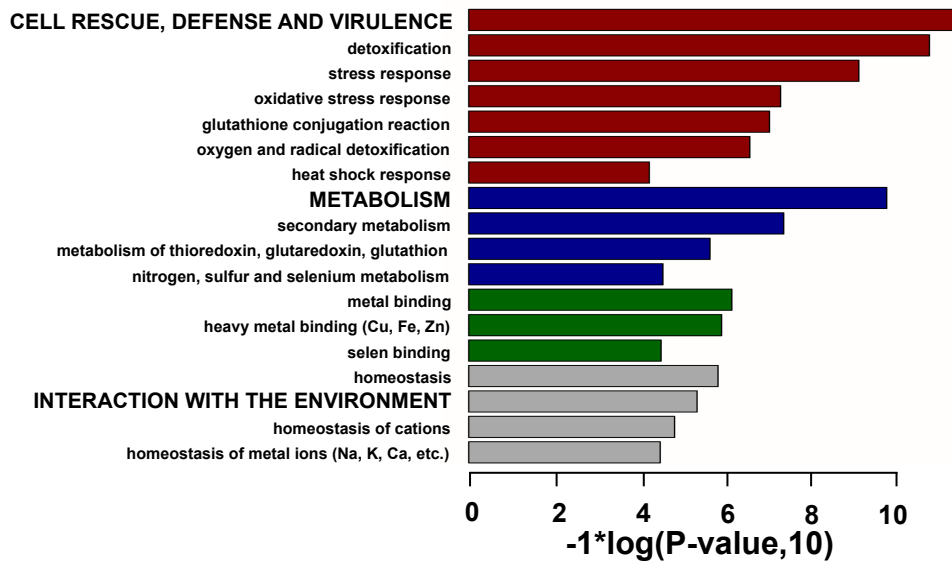
b



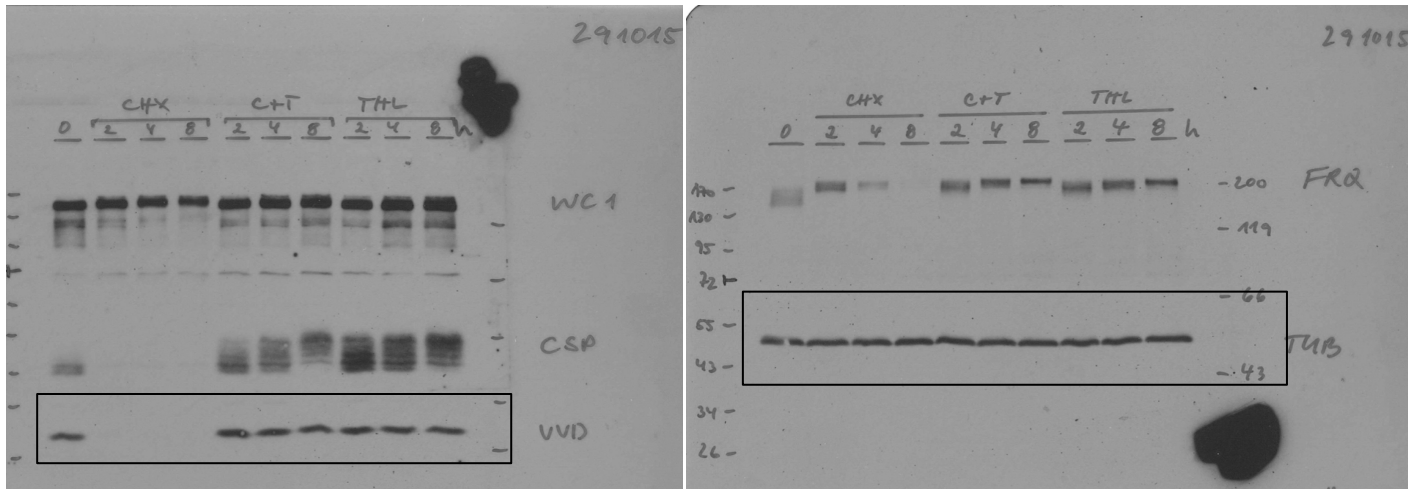
a



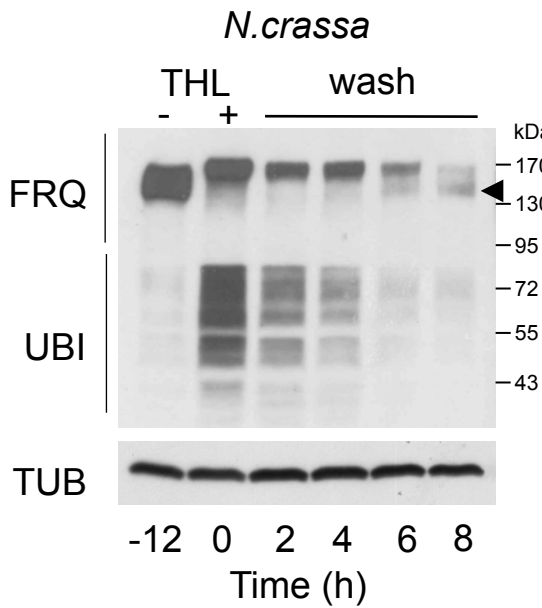
b



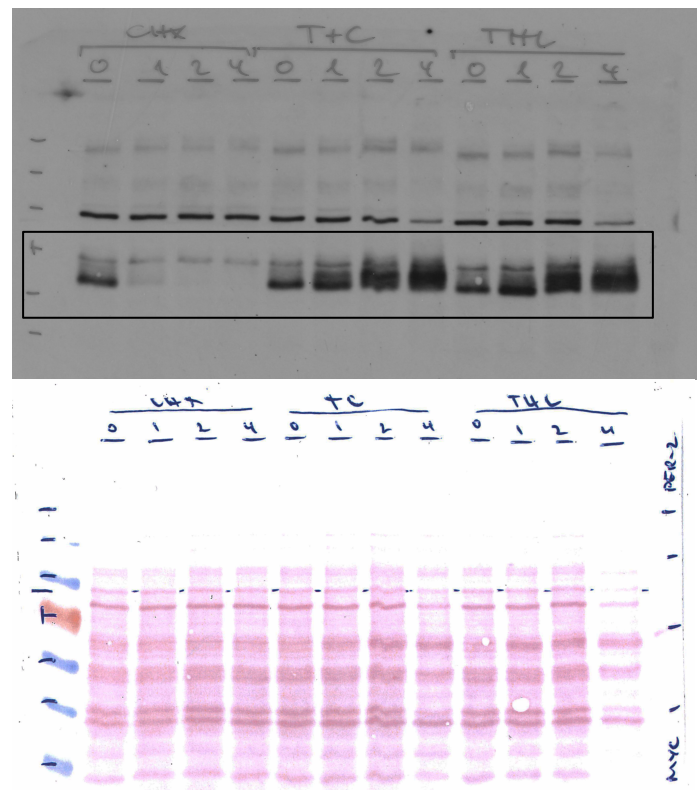
a

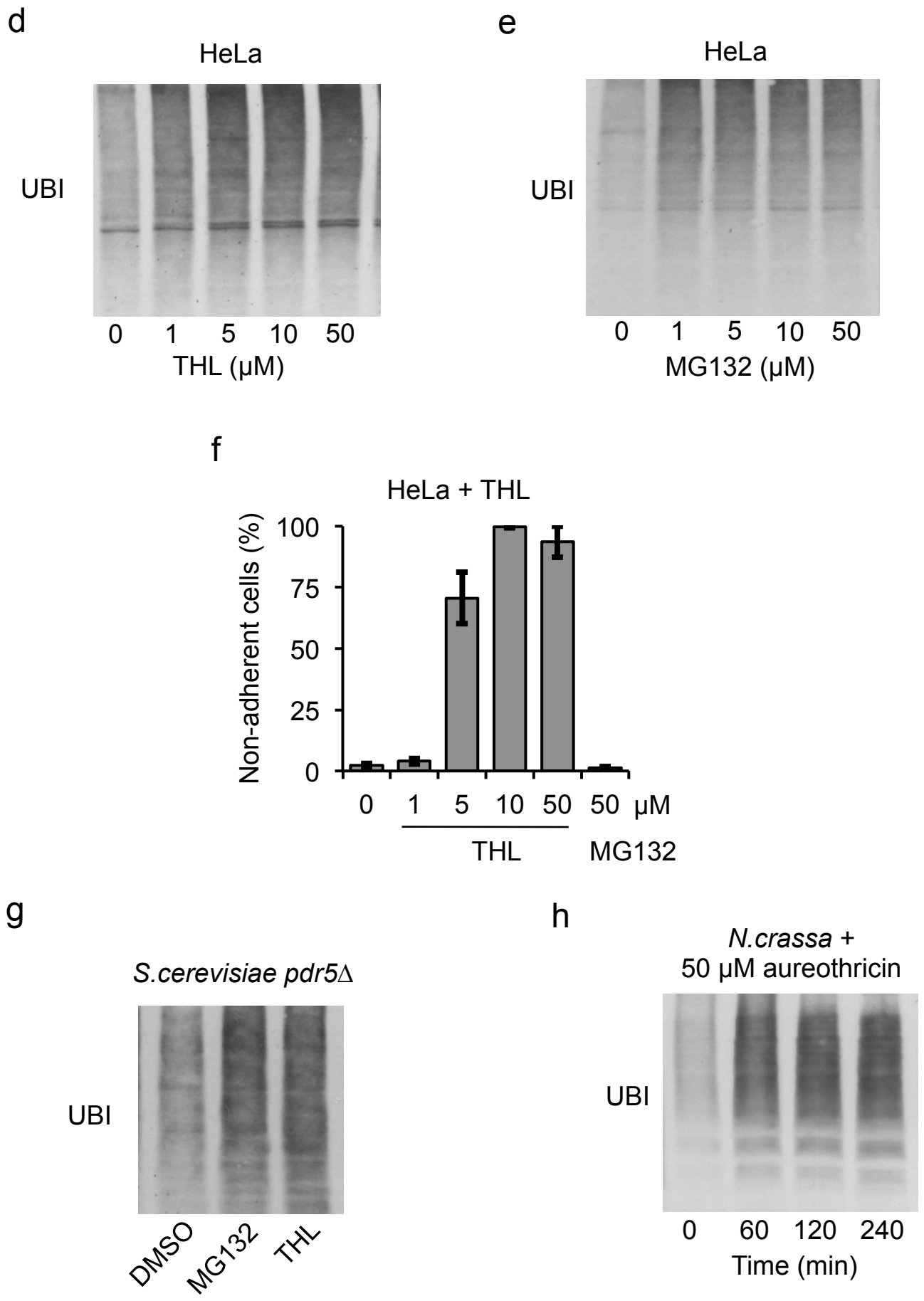


b

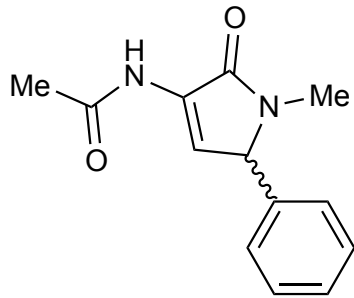


c



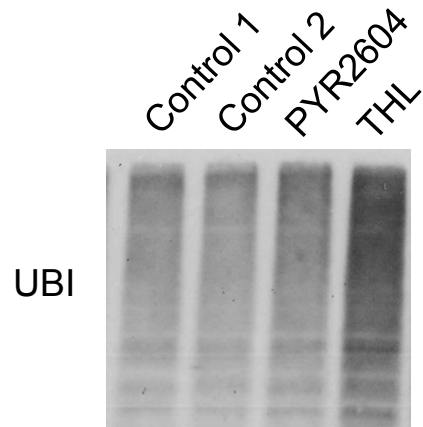


a

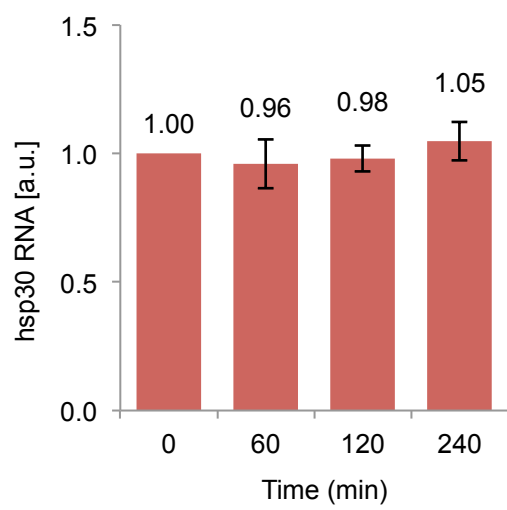
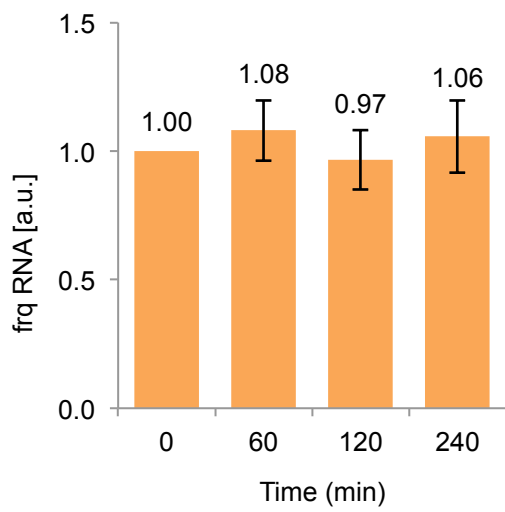


PYR2604

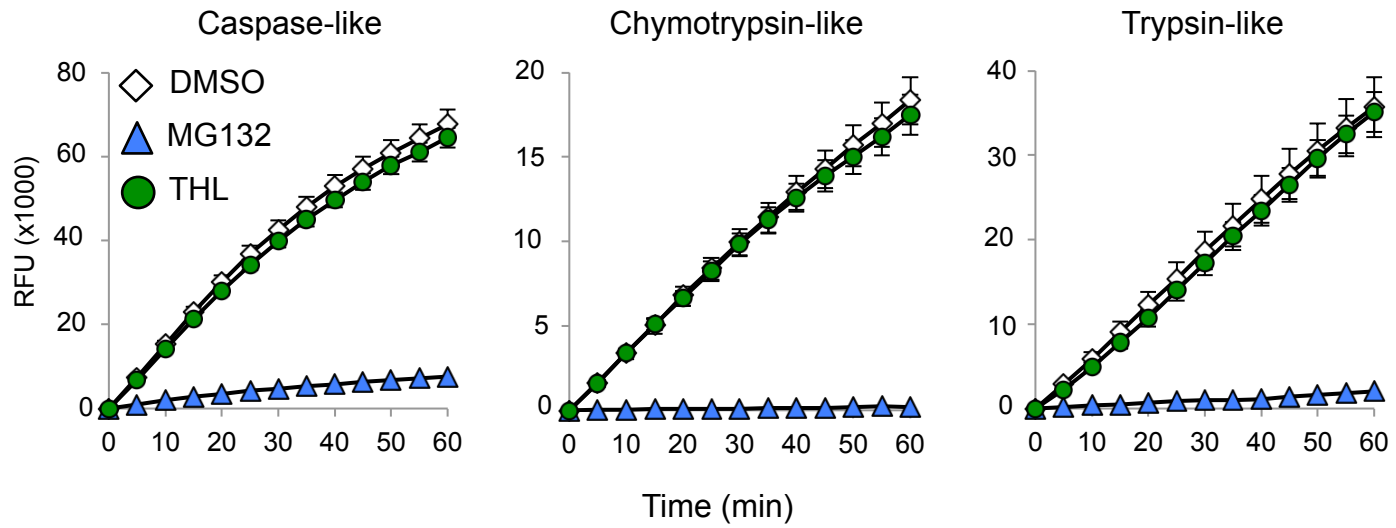
c



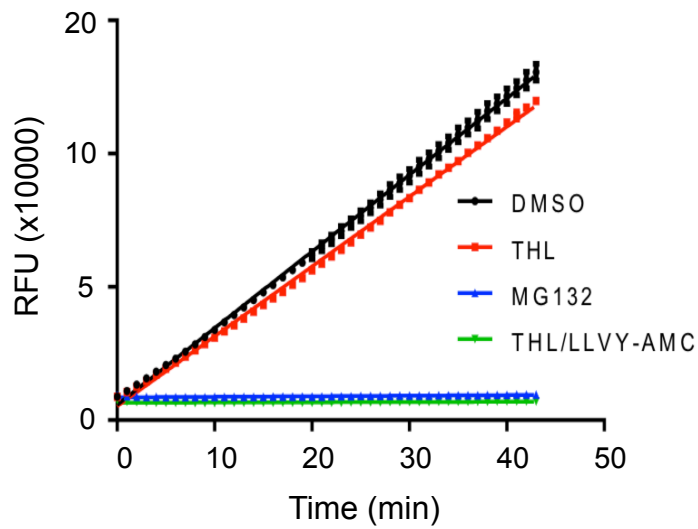
b



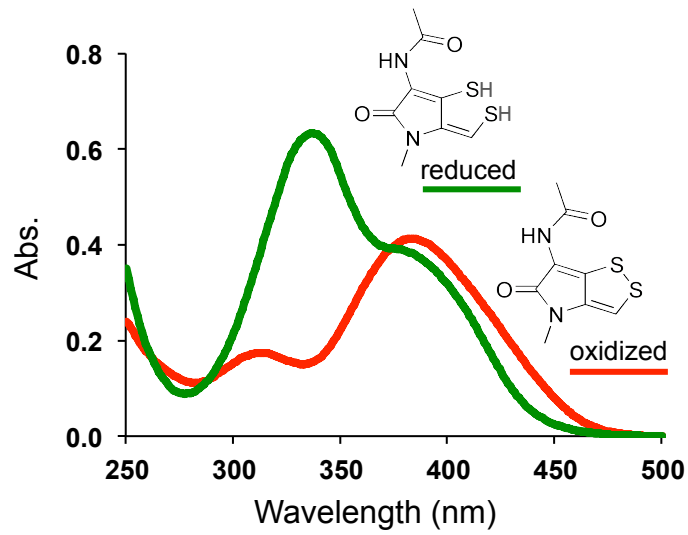
a



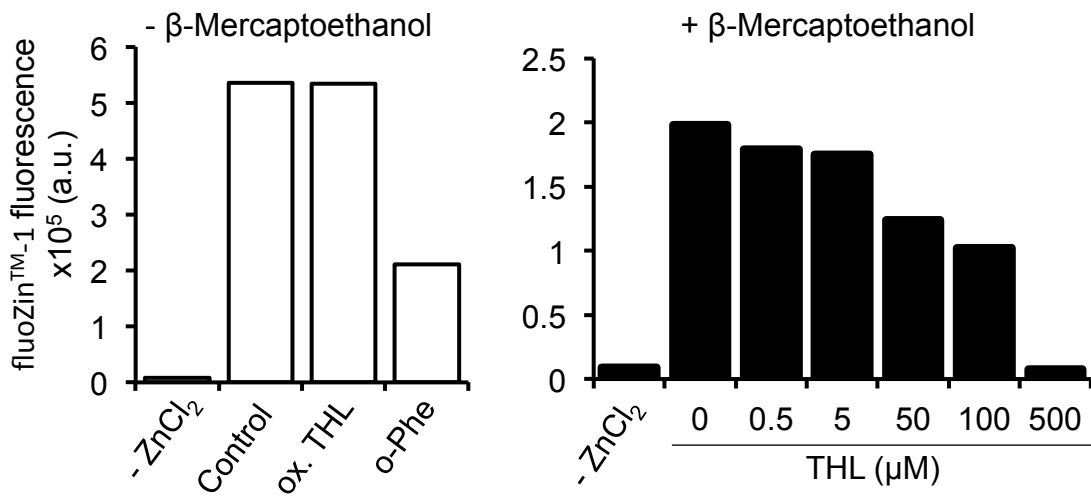
b



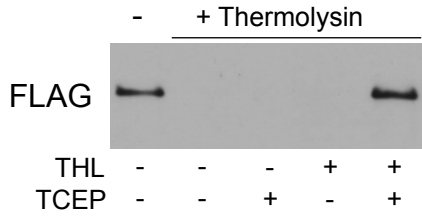
a



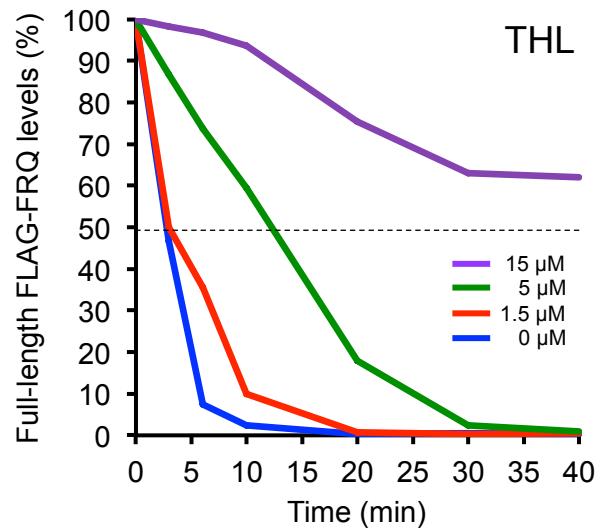
b



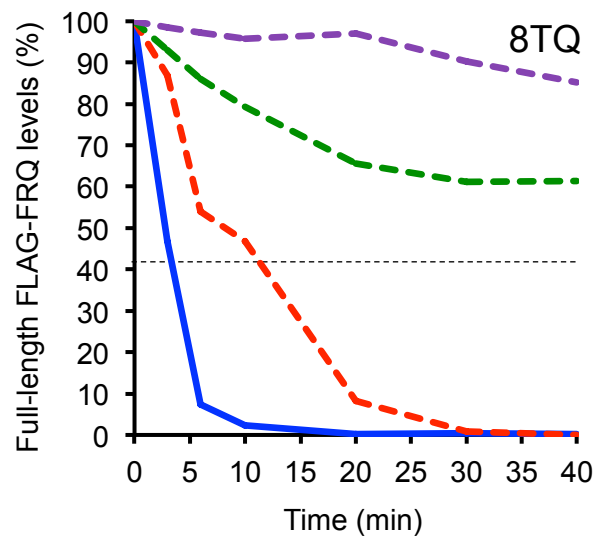
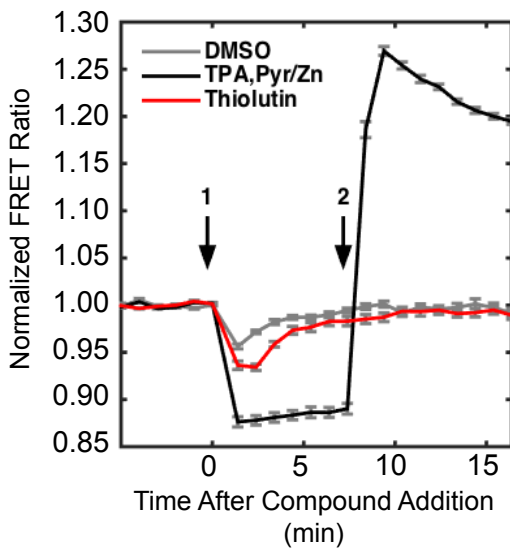
a



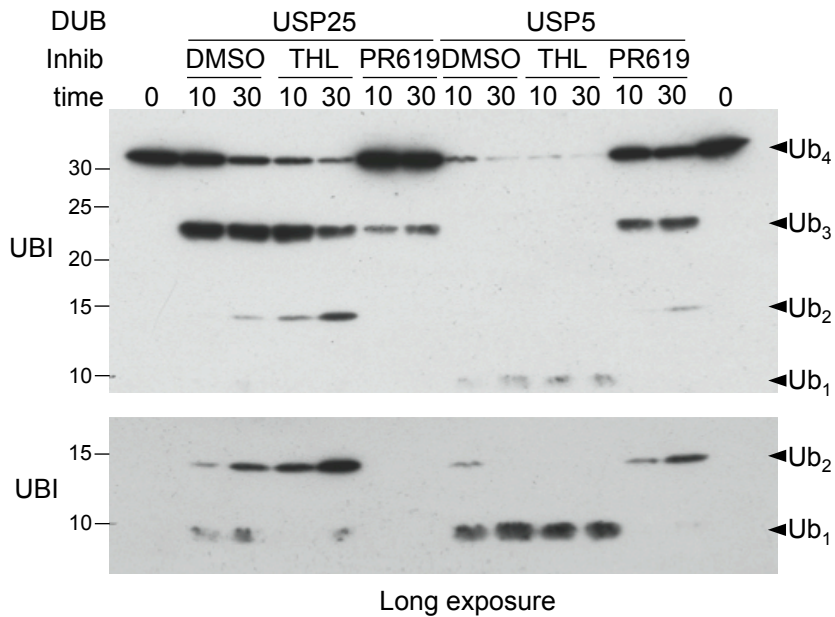
b

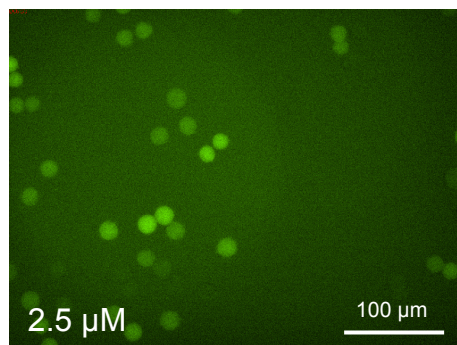
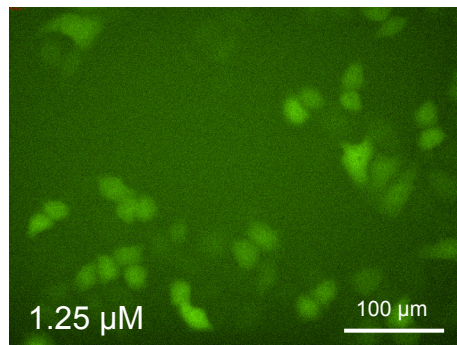
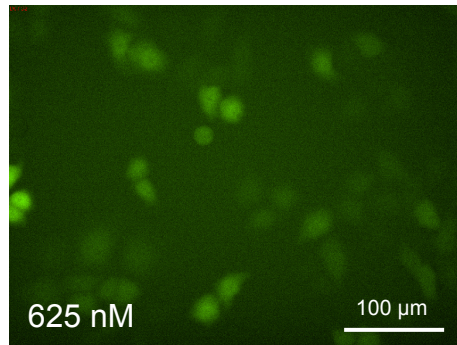
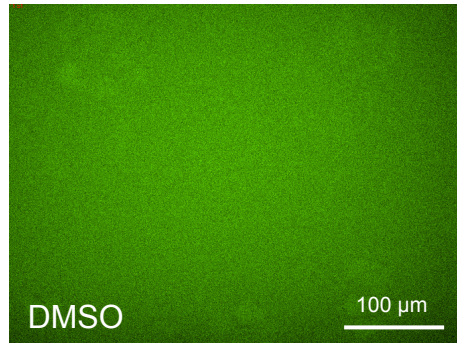


c

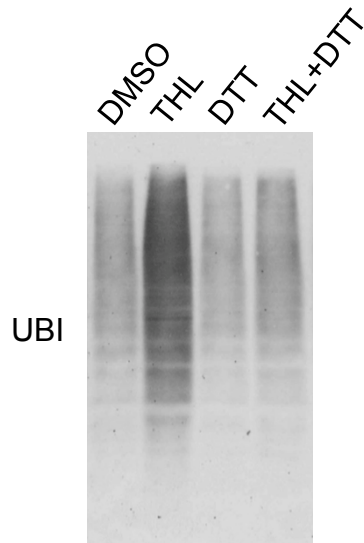


d

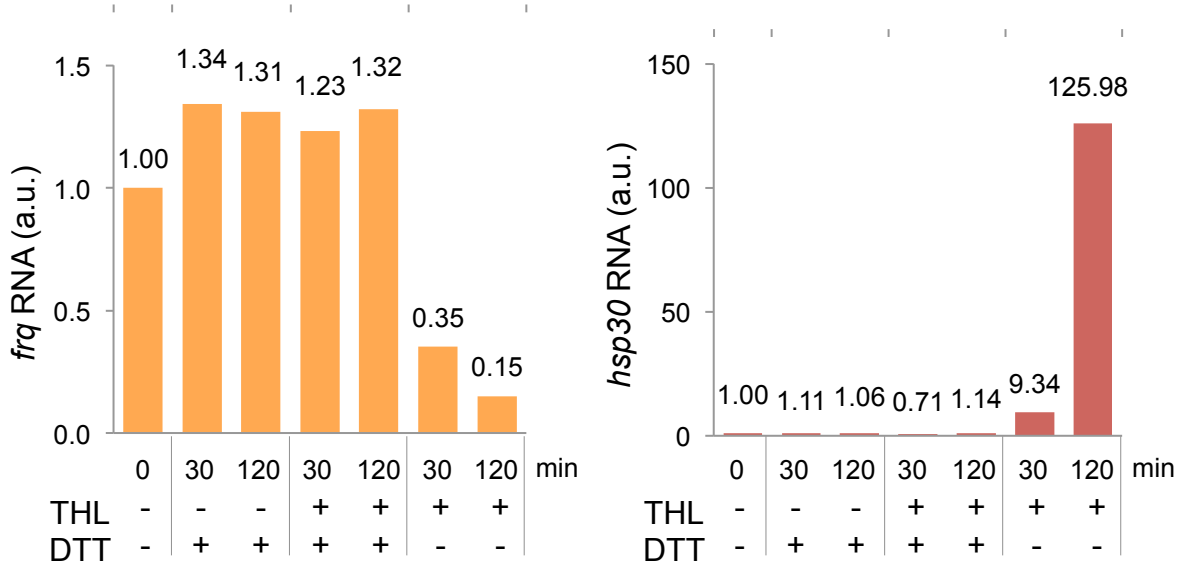




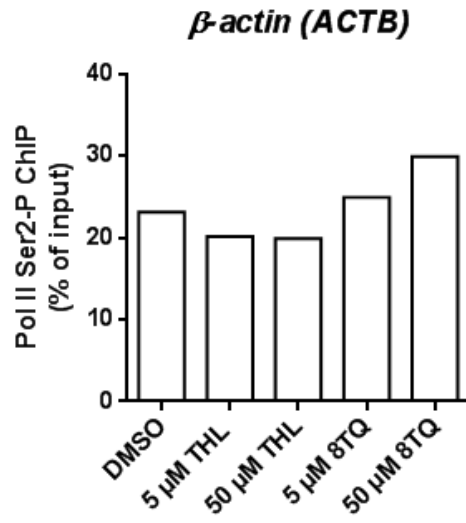
a



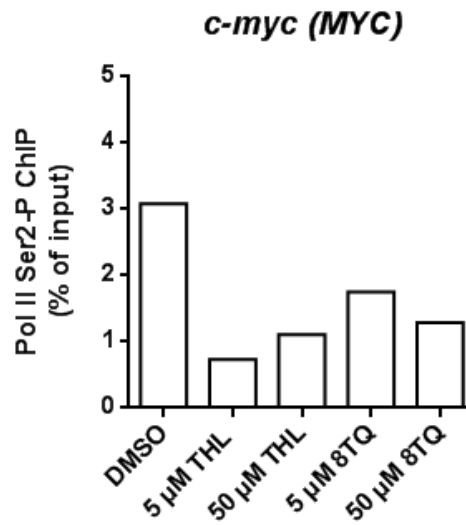
b



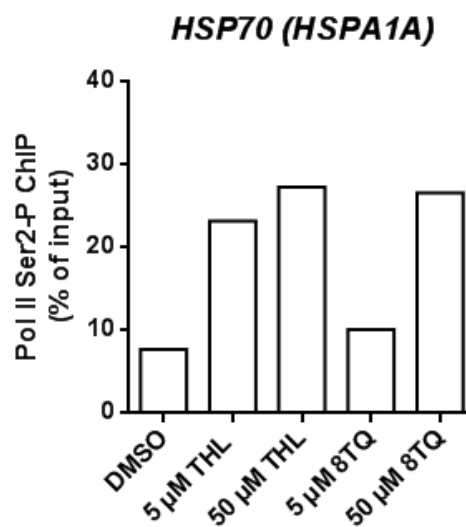
a



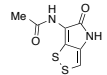
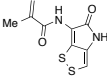
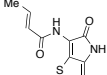
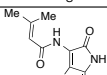
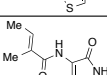
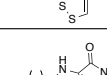
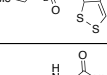
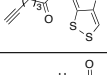
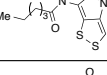
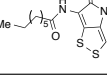
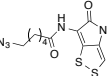
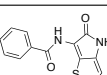
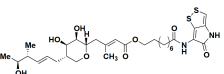
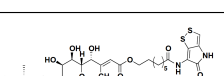
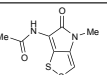
b



c



Supplementary Table

| | | RPN11 IC50 (μM) | CSN5 IC50 (μM) | AMSH IC50 (μM) | BRCC36 IC50 (μM) | Cellular IC50 (μM) |
|-----------------------------------|---|-----------------|----------------|----------------|------------------|--------------------|
| Holomycin (2) |  | 0.18 | 3.4 | 1.3 | 0.49 | 0.2 |
| Methacryloyl holothin (3) |  | 0.81 | 16.1 | 3.2 | | 0.14 |
| Crotonyl holothin (4) |  | 0.84 | 7.9 | 3.6 | | 0.13 |
| 3,3-Dimethylacryloyl holothin (5) |  | 0.5 | 1 | 1.7 | | 0.09 |
| Tigloyl holothin (6) |  | 0.57 | 1 | 1.55 | | 0.1 |
| Pentanoyl holothin (7) |  | 0.26 | 1.2 | 1.8 | | 0.12 |
| 5-hexynoyl holothin (8) |  | 0.18 | 1 | 0.61 | | 0.16 |
| Hexanoyl holothin (9) |  | 0.23 | 1.3 | 0.39 | | 0.22 |
| Octanoyl holothin (10) |  | 0.52 | 1 | 1.56 | | 0.79 |
| 6-azidohexanoyl holothin (11) |  | 0.91 | 1.9 | 0.85 | | 0.25 |
| Benzoyl holothin (12) |  | 0.2 | 2.4 | 0.9 | 0.91 | 0.32 |
| Pivaloyl Holothin (13) |  | 0.4 | 2.9 | 1 | | 0.87 |
| Pseudomonyl C holothinamide (14) |  | 0.4 | 2.6 | 0.5 | | 1.3 |
| Thiomarinol A (15) |  | 1.3 | 2.4 | 1.3 | | 0.7 |
| Thiolutin |  | 0.53 | 6.2 | 4 | 0.75 | 0.3 |

Supplementary Material

Supplementary Figure Legends

Supplementary Figure 1: Thiolutin affects transcript levels in *N.crassa* and *S.cerevisiae*

a: *N.crassa* cultures were incubated in the presence 50 μ M THL and samples were harvested after indicated time periods. Total RNA was prepared and *frq* transcripts were quantified by qRT-PCR. Data were normalized to 28S *rRNA*.

b : *S.cerevisiae* cultures ($OD_{600} = 0.5 - 0.8$) were incubated in the presence of 50 μ M THL and samples were harvested after the indicated time periods. Transcript levels of *dbp2* were quantified by qRT-PCR. Data were normalized to 18S *rRNA*. **a,b:** Error bars indicate s.d. (n=3).

Supplementary Figure 2: Thiolutin does not directly inhibit RNA polymerases

a: Uncut gel image used for Fig. 2a. Parts shown in main figure are highlighted by rectangles.

b: FunCat analysis of significantly up-regulated genes upon treatment of *N.crassa* with 50 μ M THL. Genes involved in detoxification, metal binding, heat shock and oxidative stress response are enriched in the group of up-regulated genes. Major functional categories are capitalized, and colours of the columns indicate the corresponding subcategories (not capitalized).

Supplementary Figure 3: Thiolutin inhibits the ubiquitin-proteasome system

a: Uncropped Western blots used for Fig. 3a. Parts shown in main figure are highlighted by rectangles.

b: The inhibitory effect of THL is reversible. *N.crassa* cultures were incubated for 12 h with 50 μ M THL. At time $t = 0$ mycelia were rinsed with water and transferred into fresh medium. Subsequently samples were harvested after the indicated time periods and analyzed by Western blotting with antibodies against FRQ, Ubiquitin (UBI) and β -tubulin. Note that the degradation of hyperphosphorylated FRQ that had

accumulated with THL resumed. After 6 – 8 h newly synthesized hypophosphorylated FRQ was detectable (arrowhead).

c: Uncropped Western blot and corresponding Ponceau stain used for Fig. 3b. The part shown in main figure is highlighted by a rectangle.

d, e: THL and MG132 trigger accumulation of poly-ubiquitylated proteins to a similar extent. HeLa cells were incubated for 2 h with the indicated concentrations with THL (**d**) or MG132 (**e**). RIPA extracts were analyzed by Western blotting with monoclonal Ubiquitin antibodies.

f: THL but not MG132 inhibits cell adhesion. HeLa cells were seeded densely and incubated for 24 h prior to addition of THL or MG132 at the indicated final concentrations. After 2 h the fraction of non-adherent cells (in the supernatant) was determined (n=3). Error bars indicate \pm SEM.

g: The MG132-hypersensitive yeast strain *pdr5 Δ* accumulates poly-ubiquitylated proteins with similar efficiency in the presence of THL or MG132. Yeast *pdr5 Δ* cultures (OD₆₀₀ = 0.5 – 0.8) were incubated in the presence of DMSO (control), 50 μ M THL and 50 μ M MG132, respectively and samples were harvested after 2 h. Denaturing protein extracts were prepared and analyzed by Western blotting with monoclonal Ubiquitin antibodies.

h: The dithiopyrrolone aureothricin induces accumulation of poly-ubiquitylated proteins. *N.crassa* cultures were incubated with 50 μ M aureothricin and samples were harvested after the indicated time periods. Whole cell lysates were analyzed by Western blotting with monoclonal Ubiquitin antibodies.

Supplementary Figure 4: Pyrrolone PYR2604 lacking the dithiole does not exhibit antibiotic activity

a: Structure of pyrrolone PYR2604 (**1**).

b: PYR2604 does not affect RNA levels. *N.crassa* cultures were treated with 50 μ M PYR2604 and harvested after the indicated timeperiods. Total RNA was prepared, and *frq* and *hsp30* transcript levels were quantified by qRT-PCR. Data were normalized to 28S *rRNA*. Error bars indicate s.d. (n=3).

c: PYR2604 does not induce accumulation of poly-ubiquitylated proteins. *N.crassa* cultures were incubated for 2 h with DMSO, 50 μ M PYR2604 and 50 μ M THL,

respectively and whole cell lysates were analyzed by Western blotting with monoclonal Ubiquitin antibodies.

Supplementary Figure 5: THL does not inhibit the proteolytic activity of the core proteasome

a: Proteolytic activities of the 20S proteasome are not inhibited by THL *in vitro*. Purified 20S proteasome was preincubated in the presence of DMSO, 1 μ M THL or 1 μ M MG132, respectively. Reactions were started by addition of AMC-coupled substrate (Caspase-, Chymotrypsin- or Trypsin-like, respectively) and AMC release was measured at indicated time points. Error bars indicate s.d. (n=3).

b: THL does not inhibit the chymotrypsin-like activity of the 26S proteasome. 20 μ M LLVY-AMC was incubated with 15 nM purified human 26S proteasome in the absence (black) or presence of 20 μ M THL (red) or MG132 (blue). A control experiment contains only THL and LLVY-AMC is shown in green.

Supplementary Figure 6: Reduced THL is a chelator of zinc

a: Absorption spectra of THL before (red) and after (green) incubation with 1 mM DTT. Spectra correspond to spectra of reduced and oxidized holomycin determined by mass spectrometry¹. Reduced and oxidized THL are depicted next to the curves.

b: Reduced THL binds Zn²⁺-ions. Binding of Zn²⁺ to oxidized THL (500 μ M, left panel) and reduced THL (right panel) was assayed with the fluorescent zinc-indicator fluoZinTM-1. Right panel: THL was reduced with 2.5 mM β -mercaptoethanol. Results show the average of two independent experiments measured in triplicates each.

Supplementary Figure 7: Thiolutin inhibits thermolysin but does not deplete cellular zinc

a: THL inhibits the metalloproteinase thermolysin. Recombinant FLAG-FRQ protein (100 ng) was incubated for 1h at 37°C with thermolysin (30 ng) in the presence and absence of 50 μ M of THL. 500 μ M TCEP was used as reducing agent. An equivalent of 40 ng of each sample was analyzed by Western blotting with FLAG antibodies.

b: Degradation of full-length FLAG-FRQ protein by thermolysin using THL (upper graph) and 8TQ (lower graph) at the indicated concentrations. Reactions were stopped after 3, 6 10, 20, 30 and 40 minutes, respectively, and the FLAG signal was quantified

densitometrically from western blots. Quantifications shown are the average of two independent experiments.

c: THL does not alter cellular zinc. Cells were treated with 0.5% DMSO (gray, n=11 cells), 50 μ M TPA (black, n=12 cells), or 10 μ M THL (red, n=13 cells) at the arrow.

d: THL does not inhibit USP25 and USP5 *in vitro*. Purified recombinant USP25 and USP5 were pre-incubated in SAB buffer with DMSO, 50 μ M THL and 50 μ M PR619 inhibitor for 30 min at 30°C, respectively. De-ubiquitination reaction was started by addition of 1 μ M tetra-ubiquitin chains (Ub₄). After 10 and 30 min samples were analyzed by Western blotting with monoclonal Ub antibodies.

Supplementary Figure 8: Benzoyl-holothin causes Ub-GFP accumulation without cell de-adhesion at low concentration.

Hela cells stably expressing Ub^{G76V}-GFP were treated with different concentrations of benzoyl-holothin. Images were taken after 2.5 hours. Ub^{G76V}-GFP accumulated at 0.625, 1.25 and 2.5 μ M while loss of cell adhesion (rounding up of cells) occurred at 2.5 μ M of benzoyl-holothin.

Supplementary Figure 9: Pre-reduced THL is not active *in vivo*.

a: Reduced THL does not induce accumulation of poly-ubiquitylated proteins. *N.crassa* cultures were incubated for 2 h with DMSO, 50 μ M THL, 2 mM DTT, and 50 μ M THL + 2 mM DTT (pre-incubated for 30 min), respectively. Whole cell lysates were analyzed by Western blotting with monoclonal Ubiquitin antibodies.

b: Reduced THL does not affect RNA levels. *N.crassa* cultures were treated as in (a) and harvested after 30 and 120 min. Total RNA was prepared, and *frq* and *hsp30* transcript levels were quantified by qRT-PCR. Results show the average of two independent experiments each measured in triplicates.

Supplementary Figure 10: THL and 8TQ indirectly affect transcription in gene specific manner.

Confluent HeLa cells were incubated for 40 min with 0.5% DMSO (control), 5 μ M and 50 μ M THL or 5 μ M and 50 μ M 8TQ. Cells were harvested and subjected to ChIP with antibodies against the serine 2-phosphorylated heptad repeat of the C-terminal domain of the largest subunit of RNA Pol II. Pol II Ser2P occupancy of (a)

β -actin, (b) *c-myc*, and (c) *HSP70* was determined by qPCR. Mean values from two independent experiments are shown.

Supplementary table:

Activity of holomycin derivatives. *In vitro* inhibition of Rpn11, Csn5, AMSH and Brcc36 and accumulation of Ub^{G76V}-GFP in living cells (cellular IC₅₀) are listed.

References

1. Li, B. & Walsh, C.T. Streptomyces clavuligerus HlmI is an intramolecular disulfide-forming dithiol oxidase in holomycin biosynthesis. *Biochemistry* **50**, 4615-22 (2011).